AGU PUBLICATIONS

JGR

Journal of Geophysical Research: Earth Surface

RESEARCH ARTICLE
10.1002/2015JF003705

Key Points:
- Subtle changes in water pressure cause piracy from one subglacial water catchment to another
- Flow paths across overdeepenings are most sensitive to subglacial rerouting
- Water piracy may modify the spatial patterns of ice speedup and catchment water budget

Supporting Information:
- Supporting Information S1

Correspondence to:
W. Chu,
wchu@ldeo.columbia.edu

Citation:
Chu, W., T. T. Creyts, and R. E. Bell (2016), Rerouting of subglacial water flow between neighboring glaciers in West Greenland, *J. Geophys. Res. Earth Surf.*, *121*, doi:10.1002/2015JF003705.

Received 29 DEC 2014
Accepted 15 APR 2016
Accepted article online 21 APR 2016

Rerouting of subglacial water flow between neighboring glaciers in West Greenland

Winnie Chu[1], Timothy T. Creyts[2], and Robin E. Bell[2]

[1]Department of Earth and Environmental Sciences, Columbia University, New York City, New York, USA, [2]Lamont-Doherty Earth Observatory, Columbia University, Palisades, New York, USA

Abstract Investigations of the Greenland ice sheet's subglacial hydrological system show that the connectivity of different regions of the system influences how the glacier velocity responds to variations in surface melting. Here we examine whether subglacial water flow paths can be rerouted beneath three outlet glaciers in the ablation zone of western Greenland. We use Lamont-Doherty and Center for Remote Sensing of Ice Sheets of University of Kansas (CReSIS) ice-penetrating radar data to create a new ice thickness map. We then use a simple subglacial water flow model to examine whether flow paths can be rerouted and identify the topographic conditions that are sensitive to subglacial rerouting. By varying water pressures within an observationally constrained range, we show that moderate changes in pressure can cause flow paths to reroute and exchange water from one subglacial catchment to another. Flow across subglacial overdeepenings is particularly sensitive to rerouting. These areas have low hydraulic gradients driving flow, so subtle water pressure variations have a strong influence on water flow direction. Based on correlations between water flow paths and ice velocity changes, we infer that water piracy between neighboring catchments can result in a different spatial pattern of hydrologically induced ice velocity speedup depending on the amount and timing of surface melt. The potential for subglacial water to reroute across different catchments suggests that multiple hydrographs from neighboring glaciers are likely necessary to accurately ascertain melt budgets from proglacial point measurements. The relationship between surface runoff, ice dynamics, and proglacial discharge can be altered by rerouting of subglacial water flow within and across outlet glaciers.

1. Introduction

The Greenland ice sheet has been losing mass at an increasing rate over the last several decades and currently contributes 0.7–1.1 mm yr^{-1} to global sea level rise [*Shepherd et al.*, 2012; *Intergovernmental Panel on Climate Change*, 2013; *Khan et al.*, 2014]. The mass loss is due to a combination of negative surface mass balance [*Fettweis et al.*, 2011; *Box and Colgan*, 2013; *Hanna et al.*, 2013] and the increased ice discharge across grounding lines associated with faster ice flow velocities [*Rignot and Kanagaratnam*, 2006; *Joughin et al.*, 2008; *van den Broeke et al.*, 2009]. One of the mechanisms that can cause variability in ice flow velocity is through lubrication at the base of the ice sheet as melt water penetrates to the bed from the surface [*Zwally et al.*, 2002; *Bartholomaus et al.*, 2008; *Das et al.*, 2008; *Bartholomew et al.*, 2010, 2012; *Pimentel and Flowers*, 2010; *Schoof*, 2010]. Changes in basal lubrication cause daily and seasonal variations in flow velocity [*Joughin et al.*, 2008; *Hoffman et al.*, 2011; *Sole et al.*, 2011; *Sundal et al.*, 2011; *Bartholomew et al.*, 2012; *Hewitt*, 2013]. However, it is uncertain how significant the seasonal speedup events are to the overall mass loss of the glaciers, and what controls the response of different glaciers to a similar increase in surface melting.

Theoretical and observational studies have suggested that the response of glaciers to surface melting is largely determined by the evolution of the subglacial hydrological system [*Iken and Bindschadler*, 1986; *Bartholomaus et al.*, 2008; *van de Wal et al.*, 2008; *Bartholomew et al.*, 2010; *Schoof*, 2010; *Sundal et al.*, 2011]. The transition between a slow, inefficient subglacial system and a fast, efficient system can result in a different velocity response to the same supply of meltwater from the ice surface. Following the examples of mountain glaciers, the structure of the Greenland subglacial hydrological system is thought to evolve between the slow and fast forms in response to seasonal and daily variations in meltwater input [*Mair et al.*, 2002; *Bingham et al.*, 2005; *Bartholomaus et al.*, 2008]. During winter, with little input of surface meltwater, the drainage flow paths are restricted and poorly connected, yielding inefficient water transport. In spring, when surface meltwater reaches the bed, the inefficient system is unable to cope with the input leading to higher water pressures. The elevated pressures reduce the contact area between the ice and bedrock causing increased sliding and elevated ice flow velocities [*Iken*, 1981; *Iken and Bindschadler*, 1986]. Sliding allows the

subglacial flow paths to connect. The subglacial flow paths eventually channelize as increased water flow melts the overlying ice along the pathways [*Rothlisberger*, 1972; *van de Wal et al*., 2008; *Bartholomew et al*., 2010, 2011; *Schoof*, 2010; *Sundal et al*., 2011]. If meltwater discharge is steady, water pressure drops in the channels and water flows to the adjacent inefficient drainage system, increasing ice bed contact and resulting in the slowing of ice flow. For locations that have daily variations in meltwater discharge, the drainage system tunes to average conditions. During the increase of melt in the daytime, flooding causes high pressures in channels that leak water to an adjacent subglacial system. During nighttime, meltwater sources diminish and the water system drains. The net effect of the daily variations in pressure is similar to the steady case because regions of distributed high pressure are not persistent and coupling between ice and bed increases.

Variations in the flow paths are governed by the hydraulic potential with the ice surface driving flow with a much smaller component dependent on bed topography [*Shreve*, 1972]. Hydraulic potential analyses have shown that subglacial pathways have the potential to reroute in response to modest changes in surface elevation [*Wright et al*., 2008; *Karlsson and Dahl-Jensen*, 2015]. In Antarctica, competition of subglacial water between glacier catchments or water piracy has been thought to trigger the onset or shutdown of ice stream flow [*Alley et al*., 1994; *Anandakrishnan and Alley*, 1997; *Vaughan et al*., 2008; *Carter et al*., 2013]. Detailed studies of bed topography in Antarctica show that topography tends to aid in determining the direction of subglacial flow paths by adding structure to a relatively smooth ice surface [*Wolovick et al*., 2013]. Together, rerouting and water piracy can occur beneath Greenland because the catchments are not topographically constrained. This is in contrast to mountain glaciers where drainage is tightly constrained along valleys. Water piracy can impact ice flow by redistributing surface meltwater and regional water pressure [*Lindbäck et al*., 2015].

Water flow beneath Greenland may reroute in response to the variations in water pressure [*Cuffey and Paterson*, 2010]. Here we examine whether subglacial flow paths could be rerouted among three west Greenland outlet glaciers under different subglacial water pressure scenarios. Using radar-constrained topography and an analytical, steady state water flow model, we examine the sensitivity of rerouting of subglacial flow to changes in water pressures and identify critical topographic areas that control the sensitivity.

1.1. West Greenland Study Site

Our study region along the west coast of Greenland has a subglacial hydrological system that changes rapidly with highly variable and episodic surface meltwater input [*Das et al*., 2008; *Joughin et al*., 2008, 2013] (Figure 1). This region, located to the south of the fast-flowing Jakobshavn Isbræ ($>$1000 m yr^{-1}), drains three slower moving marine terminating glaciers with average velocities of 100 to 200 m yr^{-1}: Alángordliup sermia, Sarqardliup sermia, and Nordenskiöld Gletscher (hereinafter referred as Alángordliup, Sarqardliup, and Nordenskiöld). Previous studies by *Joughin et al*. [2008] and *Das et al*. [2008] examined the influence of supraglacial lake drainage on ice flow velocities. GPS instruments installed around two supraglacial lakes (white triangles in Figure 1) showed fast ($<$2 h) drainages of lakes to the base of the ice sheet caused accelerated ice flow 100 times the background velocity [*Das et al*., 2008]. Using 24 day repeated synthetic aperture radar (SAR) data, *Joughin et al*. [2008] found that the localized accelerated ice motion was short lived, and the net annual speedup was spatially uniform across the region. The spatial uniform speedup was interpreted as the presence of a well-connected subglacial hydrological system dispersed the localized changes in water pressure uniformly across the region [*Tedstone et al*., 2014]. However, using the more frequently sampled (~11 days) TerraSAR-X (TSX) observation, *Joughin et al*. [2013] found a greater spatial heterogeneity in the peak summer velocity speedup from two melt seasons. In June 2009, the greatest speedup was concentrated in the upstream region of Sarqardliup and Alángordliup above 30 km from the ice sheet margin (Figure 1b). The downstream 30 km region experienced $<$40% summer velocity speedup from the winter velocity. In contrast, the greatest summer speedup occurred in July 2010 was more spatially extensive (Figure 1b). The downstream 30 km regions of Alángordliup and Sarqardliup experienced greater speedup ($>$80% of the winter velocity). The spatially heterogeneous ice flow speedup pattern suggests a more spatially and temporally variable hydraulic interaction between the different regions of the subglacial hydrological system. In this paper, we examine the relationship between the potential routing of subglacial water and the interannual variations in the spatial pattern of ice flow velocity between 2009 and 2010.

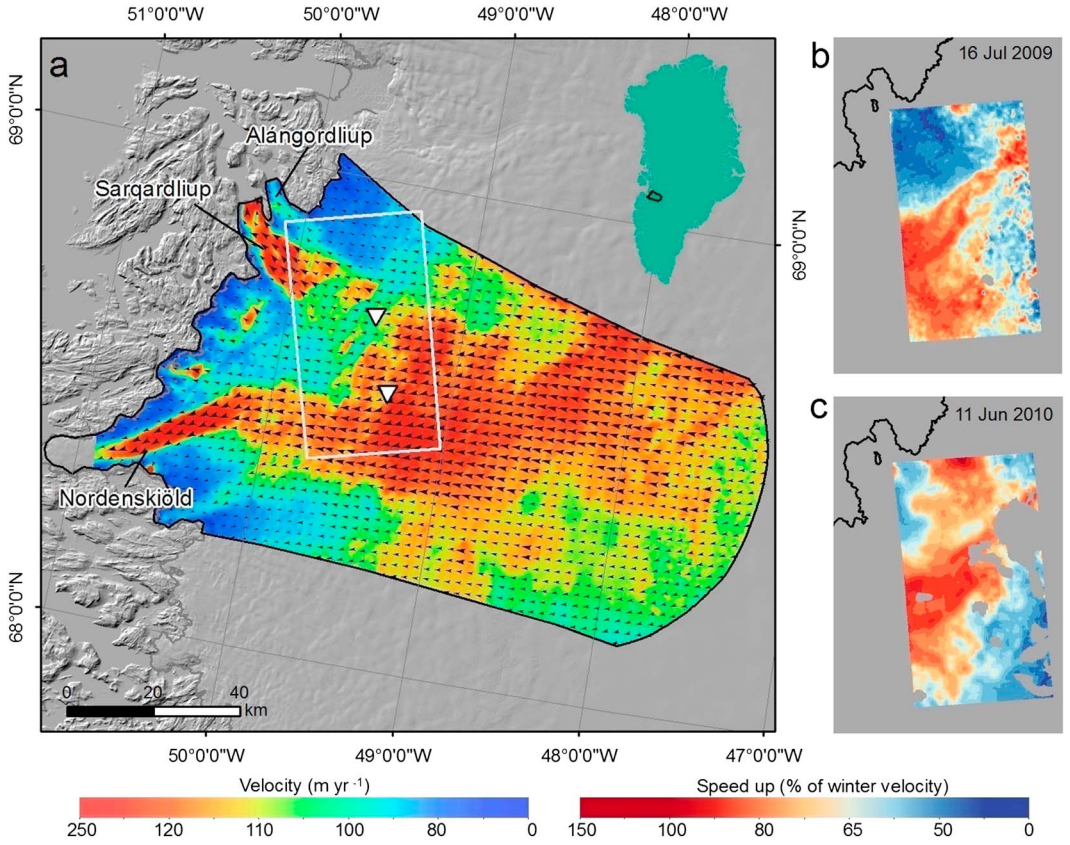

Figure 1. (a) Map of ice flow velocity from RADARSAT data collected in the winters of 2007–2008 [*Joughin et al.*, 2010]. The black arrows indicate directions of ice flow, and the color map shows speed. White triangles locate the supraglacial lakes studied by *Das et al.* [2008] and *Joughin et al.* [2008, 2013]. White rectangle shows the area displayed in Figures 1b and 1c. (b) Increase in summer 2009 flow velocity relative to winter velocity (expressed as percentage of winter speed) from TerraSAR-X data on 16 July 2009. (c) Increase in summer 2010 flow velocity relative to winter velocity on 11 June 2010 [*Joughin et al.*, 2013]. These dates are chosen to show the maximum spatial extent of the summer speedup for each year.

2. Data

The configuration of surface and bed topography largely controls the direction of subglacial water flow [e.g., *Shreve*, 1972]. For the study region, *Joughin et al.* [2013] noted that bed topography needs to be better constrained to understand the interaction between subglacial hydrology and ice flow. Using the high-resolution ice thickness data collected by Lamont-Doherty and data from the Center for Remote Sensing of Ice Sheets of University of Kansas (CReSIS), we reconstruct a new bed elevation map to examine the influence of topography on subglacial water routing. Bed elevations are calculated by subtracting the ice thickness data from a digital elevation model (DEM) of ice surface. Surface elevation is from the 30 m resolution DEM of Greenland Ice Mapping Project (GIMP) that combines ASTER (Advanced Spaceborne Thermal Emission and Reflection Radiometer), SPOT-5 (Système Pour l'Observation de la Terre), and AVHRR (Advanced Very High Resolution Radiometer) photoclinometry [*Howat et al.*, 2014].

2.1. Lamont-Doherty Survey

Ice-penetrating radar data for Sarqardliup and Alángordliup were collected using a Twin Otter aircraft in June 2008. The survey (~533 line kilometers) comprises 10 northeast-southwest trending lines spaced ~2.5 km apart, intersected by two along flow lines spaced ~10 km apart (black lines in Figure 2). The radar system, developed collaboratively with CReSIS, has a 150 MHz center pulse, a bandwidth of 10 MHz, and a transmit power of 2 kW. The system uses both a 3 μs low-gain signal and a 10 μs high-gain signal [*Gogineni et al.*, 2001; *Jezek et al.*, 2006]. The pulse repetition interval is 100 μs, and depending on the flight, velocity typically samples the ice at less than 2 m intervals in the along-track direction. The radar footprint is approximately

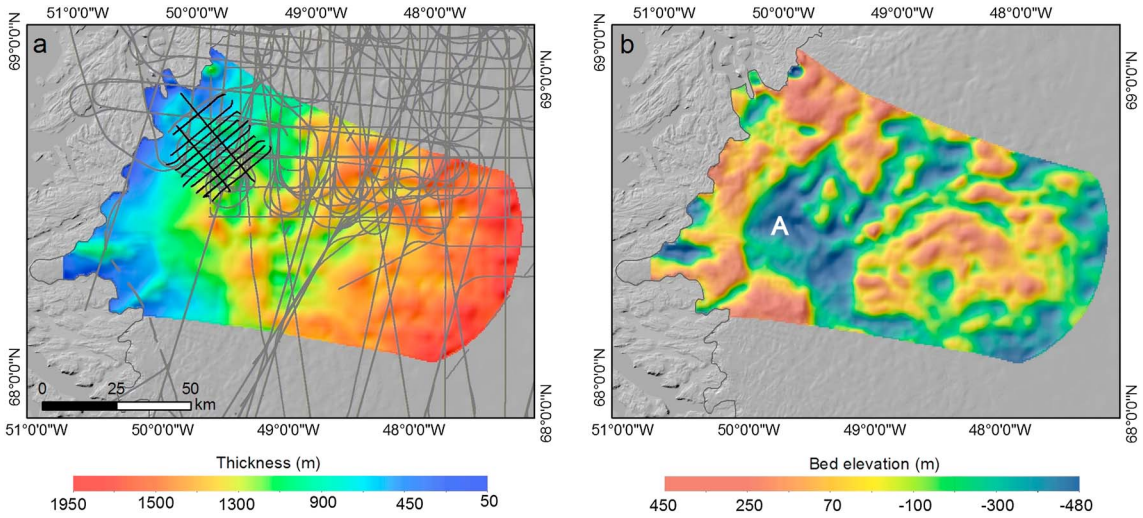

Figure 2. (a) Ice thickness map from kriging the Lamont-Doherty (black lines) and CReSIS data (grey lines). (b) Bed topography calculated from subtracting the interpolated ice thickness from the GIMP surface elevation DEM. A in Figure 2b highlights the subglacial overdeepening where major water rerouting occurs.

1 km in the cross-track direction. The low-gain and high-gain channels are combined and migrated using a 1-D synthetic aperture radar (SAR) algorithm to produce radar echograms [*Hélière et al.*, 2007]. The ice thickness is picked using a hybrid manual-automatic system along the sharpest vertical gradient of the radar signal [*Wolovick et al.*, 2013]. A crossover analysis of the Lamont-Doherty thickness data gives a mean instrumental error of ±14 m ($N = 20$) (Figure 3a).

2.2. CReSIS Survey

The majority of the ice thickness data in this study were acquired by CReSIS (https://data.cresis.ku.edu/data/rds/) [*Gogineni et al.*, 2001]. We use the radar-sounding data collected by a series of instruments from 1999 to 2013 to compile the new ice thickness data set (grey lines in Figure 2). Most of the data (62%) were collected between 2010 and 2013 by the Multi-Channel Coherent Radar Depth Sounder (MCoRDS). Approximately 34% of the data are from 2003 to 2005 acquired by the Advanced Coherent Radar Depth Sounder (ACORDS). The remaining 4% are from 2006 to 2009 collected by the Multi-Channel Radar Depth Sounder (MCRDs) and from

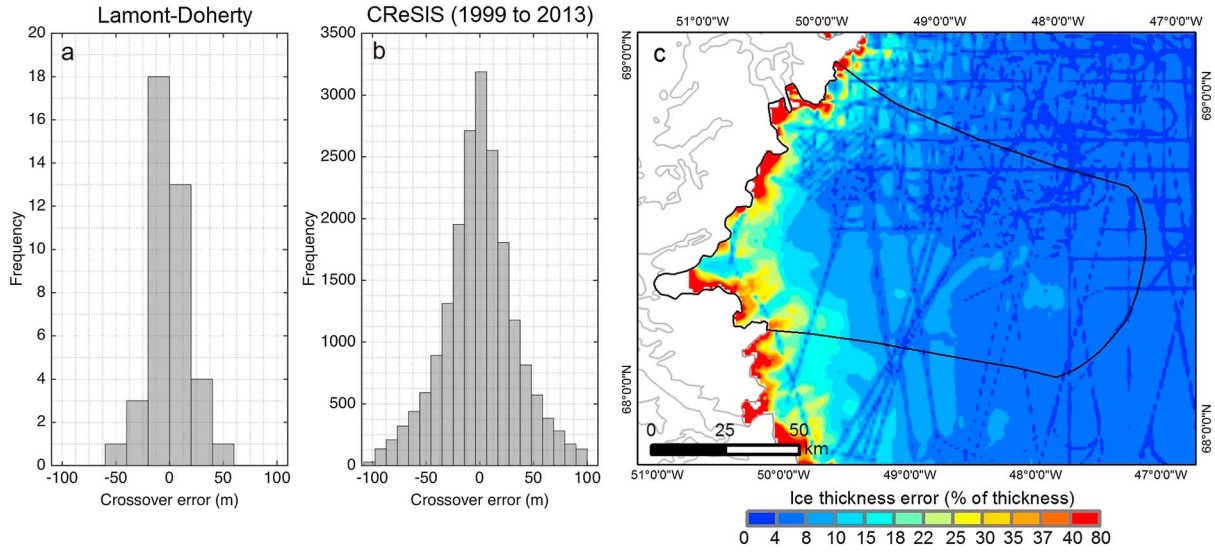

Figure 3. Crossover errors in ice thickness from (a) the Lamont-Doherty data and from (b) the CReSIS data. (c) Interpolation errors in ice thickness across the catchment expressed in term of percentages of ice thickness.

1999 to 2002 by the Improved Coherent Radar Depth Sounder (ICORDS). These data have an average track spacing of ~10–20 km, spanning a region about 290 km north-south by 65 km east-west. The ice thickness measurements have a nominal precision of ±10 m [*Gogineni et al.*, 2001]. The actual accuracy of the data varies with location and the quality of the radar picks. The primary error sources are system electronic noise, multiple reflections, and off-nadir scattering from the presence of crevasses, water, and rock outcrops. Other error sources include the uncertainties in the correction for firn depth and in the dielectric properties of ice. A crossover analysis of the CReSIS data yields a mean instrument error in thickness of ±42 m ($N = 10{,}945$) for the study region (Figure 3b).

3. Methods

3.1. Interpolation of Topography

The Lamont-Doherty and CReSIS ice thickness data are interpolated to a regular grid using ordinary kriging [*Deutsch and Journel*, 1997]. Ordinary kriging estimates thickness $H(x, y)$ at a given location using nearby measurements, H_i, with a discrete spatial weighting function, $\lambda_i(x, y)$ assigned according to the elevation covariance, so that

$$H(x, y) = \sum_{i=1}^{n} \lambda_i(x, y) H_i, \tag{1}$$

with n representing the nearest 100 measurements within a radius of 50 km. Ordinary kriging assumes that the mean of the data points is unknown but constant and requires the weights to sum to 1,

$$\sum_{i=1}^{n} \lambda_i(x, y) = 1. \tag{2}$$

The weights are calculated to minimize the variance of the estimation error. The spatial covariance of the measurements is derived from an exponential semivariogram model. We find a best fit between the model and measurements with a variogram of a sill of 24 km, a range of 1.5 km, and a nugget of 35 m. The sill represents the variance of the ice thickness measurements. The range represents the distance limit beyond which the ice thickness data are no longer correlated. The nugget was given by the mean measurement errors of the Lamont and CReSIS data. The thickness data are interpolated to a regular Cartesian grid with 500 m spacing. Bed elevation is derived by subtracting the ice thickness grid from the GIMP ice surface DEM [*Howat et al.*, 2014].

3.2. Error Analysis

A reliable estimate of the error in the DEMs is crucial to assess the uncertainty in the subglacial hydrological potential. The two primary sources of error are from the ice thickness observations and the interpolation error. Observation errors are constrained by a crossover analysis of the ice thickness data set that includes both the Lamont-Doherty and CReSIS thickness described previously. A total of 10,965 crossover differences are calculated, and the mean observation error in thickness is 31 m. The histograms of thickness crossover differences from the two campaigns are shown in Figures 3a and 3b. The GIMP ice surface DEM contributes ±10 m of uncertainty.

The interpolation error in the ice thickness DEM depends on point density of the observations and variability of the measured ice thickness. We estimate this uncertainty using a standard statistical error analysis, bootstrapping [*Cressie*, 1993; *den Hertog et al.*, 2006; *Bamber et al.*, 2013]. We calculate the interpolation error by removing an observation from the data set and using the remaining data to interpolate the value at the observation location. Using the known observation value at this location, the interpolation error is represented by the difference between the interpolated and observed values. The observation is then returned into the data set, and the process is repeated for all of the 5,427,487 observations to obtain a mean interpolation error at individual locations shown in map view in Figure 3c.

Interpolation errors at points far from the data lines dominate the uncertainty in the bed. Figure 3c shows that the largest errors are in the southern region where the flight line spacing are about 40 km apart. Because of the sparsity of data, the ice thickness of Nordenskiöld is poorly constrained with an averaged error in thickness of 80 m. In contrast, in regions near Sarqardliup and Alángordliup the errors are significantly

smaller with an averaged error of 20 m because of the dense data coverage provided by the 2.5 km spaced Lamont tracks and the ~10 km spaced CReSIS tracks. Thus, the influence of the error in DEMs on the subglacial water flow paths should be smaller in the regions near Sarqardliup and Alángordliup relative to Nordenskiöld. The impact of error in DEMs on water flow is examined in section 4.3.

3.3. Subglacial Flow Path and Catchment Delineation

To examine how the predicted routing of subglacial water flow responds to a change in the regional water pressure, we use the gridded topography product with a subglacial water flow model to calculate flow paths and catchment areas for a range of pressure values. The water flow model follows a Darcian-type formulation where water flux, Q, flows down the hydraulic potential gradient, $\nabla\phi$, according to

$$Q = -k\nabla\phi, \tag{3}$$

where k is the hydraulic conductivity of the subglacial hydrological system. Similar hydraulic potential analysis has been applied in Greenland [*Lewis and Smith*, 2009; *Banwell et al*., 2013; *Livingstone et al*., 2013; *Karlsson and Dahl-Jensen*, 2015] and Antarctica [*Wright et al*., 2008; *Wolovick et al*., 2013; *Creyts et al*., 2014] to estimate subglacial drainage flow paths. Following the *Shreve* [1972] formulation, $\nabla\phi$ is calculated from

$$\nabla\phi = \rho_w g\nabla z_b + \nabla P_w = \rho_w g\nabla z_b + \nabla P_i - \nabla N, \tag{4}$$

where ρ_w is the density of water, g is gravitational acceleration, z_b is the elevation of the bed, P_w is water pressure, P_i is ice overburden pressure, and N is effective pressure defined as the difference between ice overburden pressure and water pressure $N = P_i - P_w$. The effective pressure gives a measure of how the water system is pressurized relative to ice overburden. We continue to simplify equation (4) by introducing the ice thickness as the difference in ice surface elevation and bed elevations: $H = z_s - z_b$, so that

$$\nabla\phi = \rho_w g\nabla z_b + \rho_i g\nabla H - \nabla N. \tag{4b}$$

Following earlier studies [e.g., *Willis et al*., 2012; *Banwell et al*., 2013], we use the simplification of *Shreve* [1972] to group effective pressure into the ice overburden pressure using a prefactor f, called the flotation fraction on the water pressure $P_w = fP_i$,

$$f(\rho_i g\nabla H) = \rho_i g\nabla H - \nabla N, \tag{4c}$$

so that

$$\nabla N = (1 - f)\rho_i g\nabla H. \tag{4d}$$

Formally defined, f is the ratio of water pressure to ice overburden pressure, $f = P_w/P_i$. In this case, $f < 1$ indicates that the water pressure is below the ice overburden pressure, $f = 1$ indicates that the water pressure is at the ice overburden pressure, and $f > 1$ means that water pressure is above the ice overburden pressure. A natural lower boundary for the pressures is limited by atmospheric pressure ($f = 0$). The other natural condition is slightly overpressured ($f = 1.11$) based on the difference of the densities of water and ice where a crevasse or moulins could be filled to the ice sheet surface and effective pressures would be modestly negative.

The final form of the hydraulic gradient is

$$\nabla\phi = \rho_w g\nabla z_b + f\rho_i g(\nabla z_s - \nabla z_b), \tag{5}$$

with $\rho_w = 1000\ \mathrm{kg\ m^{-3}}$, $\rho_i = 917\ \mathrm{kg\ m^{-3}}$, and $g = 9.8\ \mathrm{m\ s^{-2}}$.

We calculate the hydraulic potential surfaces for a range of flotation fraction values defined by these natural boundaries. Similar to a previous study by *Flowers and Clarke* [1999], we run a $D\infty$ routing algorithm [*Tarboton*, 1997] on the hydraulic potential surfaces to calculate water flow paths and delineate catchment area. We estimate subglacial flow paths assuming that the flotation fraction value varies between the limits of 0.6 to 1.11 to examine the sensitivity of flow paths to changes in water pressure. The flotation limit is selected based on the observations of the evolution of subglacial water pressures in southwest Greenland [*Meierbachtol et al*., 2013; *Andrews et al*., 2014] and in alpine glacier environments [*Iken and Bindschadler*, 1986; *Iken and Truffer*, 1997; *Sugiyama and Gudmundsson*, 2004; *Harper et al*., 2005; *Fudge et al*., 2009]. While alpine glaciers may not be a perfect analog to Greenland [*Hoffman et al*., 2011], they provide annual records of subglacial water pressure that are currently absent for Greenland.

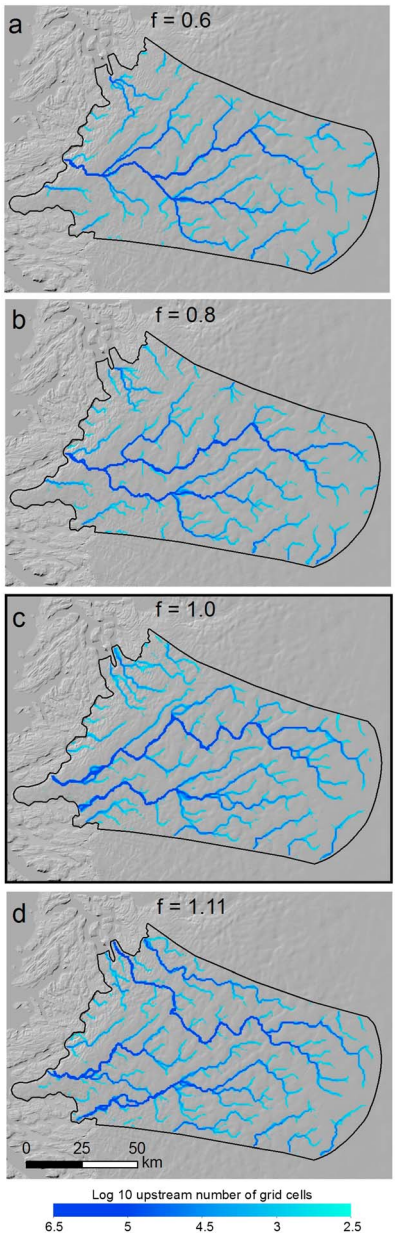

Figure 4. Subglacial water flow paths (blue lines) for the three glaciers assuming a flotation fraction of (a) $f = 0.6$, (b) $f = 0.8$, (c) $f = 1.0$, and (d) $f = 1.11$.

The range of flotation fraction values represents a modest spectrum from relatively low water pressure where the subglacial system likely channelizes to an overpressured state where water would distribute across the bed. Exact morphological transitions are absent from our study because they would require the use of more sophisticated models [*Creyts and Schoof*, 2009; *Pimentel and Flowers*, 2010; *Schoof*, 2010; *Hewitt*, 2013; *Werder et al*., 2013]. Because the purpose of this paper is to examine the interaction of subglacial flow paths with topography, we choose to use a simpler, analytical model that can include realistic topography to calculate water flow paths. Similar analytical water models have been applied elsewhere in Greenland, and the calculated flow paths are considered to represent the long-term steady state configuration [*Hagen et al*., 2000; *Ahlstrøm et al*., 2005; *Willis et al*., 2012; *Banwell et al*., 2013].

4. Results

4.1. Flow Paths Change With Water Pressure Conditions

Our results show how subglacial flow paths are rerouted when a moderate change in the flotation fraction is applied uniformly across the study region. The response of individual pathway varies from minor adjustments to the flow tributaries within the ice catchment to a major rerouting that causes piracy between neighboring glaciers. For our study region, we find that when the flotation fraction varies from 0.6 to 1.0, a minor adjustment occurs in the small hydrologic tributaries (Figure 4). However, when the catchment is overpressured to a flotation fraction of 1.11, major rerouting of water pathways occur and piracy between neighboring catchments ensures (Figure 5).

For $f = 0.6$ to 1.0, Nordenskiöld receives the majority of the subglacial water draining from the upstream catchment farther than 60 km from the ice sheet margin (Figures 4a to 4c). In contrast, Sarqardliup and Alángordliup have confined subglacial catchment areas that receive water mainly from the downstream regions within 30 km from their termini. Subglacial water that drains from the upstream regions is diverted away by the adverse slope along the bed that aligns parallel to the coast to roughly 30 km from the glacier termini (Figure 5a). Instead of draining through the downstream regions of Sarqardliup and Alángordliup, this upstream water is transported toward Nordenskiöld along the subglacial overdeepening (A in Figure 2b).

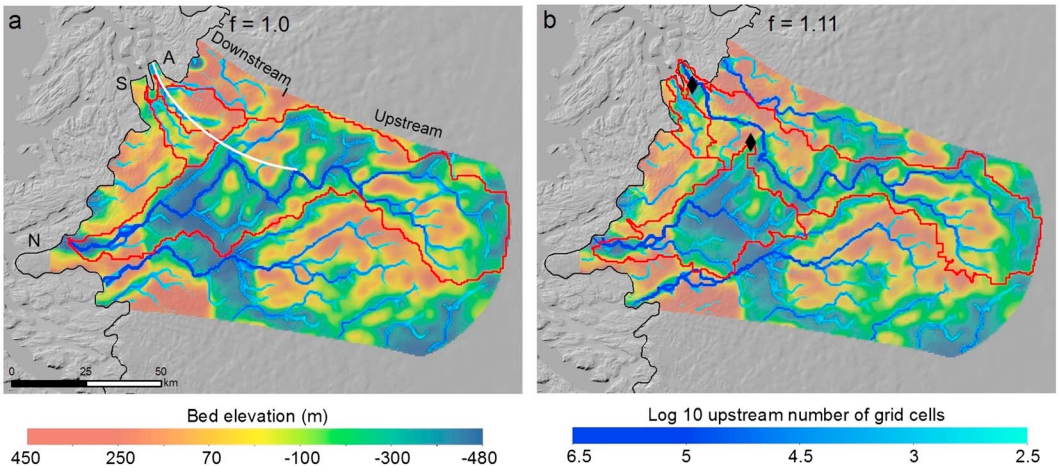

Figure 5. Flow paths from Figure 4 with the spatial extent of subglacial water catchment (red polygons) overlaid on the bed topography. The black diamonds highlight the regions where water reroutes with a 10% increase of flotation fraction. The white line shows the location of the along-flow profile in Figure 6. (a) For the flotation example where the system is at the ice overburden pressure ($f = 1.0$), Nordenskiöld receives most of the water in the region. (b) This contrasts sharply with the flotation example at $f = 1.11$ where Alángordliup drainage catchment captures majority of the water.

This configuration of subglacial flow paths contrasts sharply when water is overpressured and the flotation fraction is set to 1.11 (Figure 4d). At 111% of the overburden pressure, drainage pathways that previously flow along the overdeepening are rerouted to flow across the adverse-sloped bed (Figure 5b). Water is pirated from Nordenskiöld to the downstream catchment of Alángordliup. If no water is stored at the bed, this rerouting could lead to a ~30% increase in drainage discharge into the fjord of Alángordliup. While we do not expect flotation conditions to exist everywhere across the catchment, our results indicate that localized pressure in excess overburden at critical locations can cause rerouting of subglacial water (see section S3 in the supporting information). In particular, if moulins or fractures drain surface water at or upstream of these locations, we anticipate that subglacial flow paths could be rerouted up and out of the overdeepening.

4.2. Flow Dependence on Topography

The configurations of subglacial water flow paths are strongly dependent on topography [*Shreve*, 1972]. Rerouting of water flow occurs when the relative dependence on surface and bed topography is modified with changes in water pressure. When water pressure reaches flotation, equation (5) shows that the ice surface slopes are 11 times more important than bed slopes in steering flow. If the system reaches overpressure at $f = 1.11$, surface slopes dominate the water flow direction. However, the dependence of subglacial flow on surface slope reduces with lower water pressures, and bed slopes show a greater influence on the water flow direction. At $f = 0.8$, for example, bed slopes that are 2.7 times the surface slopes have equal influence on flow paths direction. At $f = 0.6$, bed slopes that exceed 1.2 times the surface slopes dominate flow direction, and the hydraulic potential surface closely mimics the variations in bed topography (Figure 6). As the water pressure drops below these thresholds, we expect subglacial flow paths to reroute as surface or bed topography becomes more important to flow direction. In the case of our study region, the water system is predicted to overcome the bed topography as the subglacial system reaches overpressure. The pressure threshold where surface slope dominates water routing varies across the catchment and depends on the local ratio of surface and bed slopes.

Because the dependence of water flow on topography changes with the flotation fraction, we find that the regions where major rerouting occurs are near subglacial overdeepenings, locations of local closed depressions with bed slopes reversed with respect to the surface slopes. An example is the overdeepening beneath Nordenskiöld and Sarqardliup at ~30–50 km from the ice sheet terminus (A in Figure 2b). A similar but less significant rerouting occurs in the adverse-sloped bed at ~10 km from the terminus where subglacial flow paths are predicted to reroute between Sarqardliup and Alángordliup (black diamonds in Figure 5b).

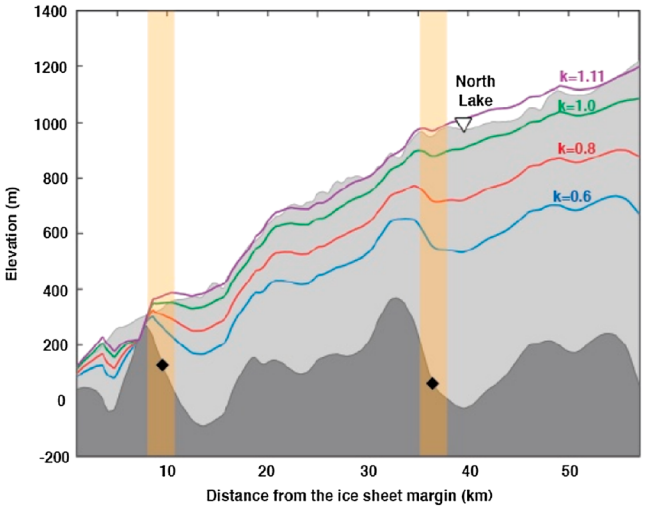

Figure 6. Along-flow profile for Alángordliup across the regions of rerouting of subglacial water flow paths (black diamond). The rerouting locations are shown in relation with the surface and bed topography (shaded patch), and the supraglacial lake (North Lake) studied by *Das et al.* [2008] and *Joughin et al.* [2008, 2013] (white triangle). Hydraulic head surfaces for different assumptions of flotation fractions are also shown to illustrate the increasing dependence of water flow on bed topography at lower flotation fractions (colored lines).

Another reason that subglacial rerouting is more likely to occur in overdeepened areas is that the adverse-sloped bed flattens the gradient of hydraulic potential across the region [*Creyts et al.*, 2013, 2014]. A flatter potential gradient surface is more prone to changes for a smaller perturbation in the water pressure [*Cook and Swift*, 2012; *Creyts et al.*, 2013]. Overdeepenings also tend to be regions that have water pressures close to or slightly above flotation [*Hooke and Pohjola*, 1994; *Lawson et al.*, 1998]. An addition of surface water such as from a supraglacial lake drainage event could elevate pressures farther. In the melt season when lake drainage events occur, overdeepenings may frequently reach superflotation pressures that could potentially cause water piracy between Nordenskiöld and Alángordliup. This piracy between the two catchments would depend on the timing of lake drainages as well as the seasonal development of the subglacial hydrological system. Because overdeepenings tend to have flatter ice surface slopes [*Gudmundsson*, 2003; *Cook and Swift*, 2012], supraglacial lakes form preferentially near these regions where the subglacial system is sensitive to rerouting [*Echelmeyer et al.*, 1991; *Sergienko*, 2013]. The supraglacial lake studied by *Das et al.* [2008] (North Lake) is located at ~5 km upstream from the subglacial overdeepening where rerouting between Nordenskiöld and Alángordliup is predicted to occur at pressures in excess of flotation (Figure 6). If the drainage of this lake causes the subglacial water pressure to exceed flotation, then our findings predict that the meltwater would be transported to Alángordliup. In contrast, if

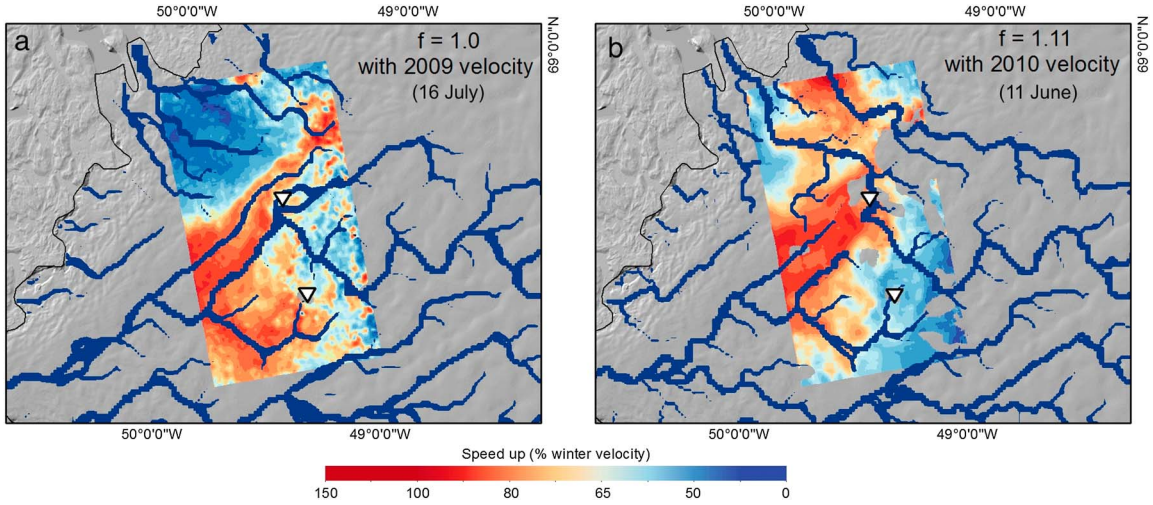

Figure 7. Subglacial water flow paths (dark blue lines) for two flotation examples, at flotation and overpressure, overlain with the observed ice velocity speedup for 2009 and 2010 summer and the two supraglacial lakes studied by *Das et al.* [2008] and *Joughin et al.* [2008] (white triangles). (a) Flow paths for $f = 1.0$ with the 16 July 2009 summer speedup. (b) Flow paths for $f = 1.11$ with the 11 June 2010 summer speedup. The additional water along the base of Alángordliup due to rerouting may have contributed to the higher velocities in the lower catchment in 2010.

the drainage occurs when pressure is below flotation, then the water would instead be delivered to Nordenskiöld (Figure 7). We suggest that therefore, the rapid supply of surface meltwater to an underdeveloped subglacial drainage system may trigger the catchment-scale rerouting of subglacial water pathways.

4.3. Influence of Error in DEMs on Flow Paths

Because relatively small changes in water pressure may result in the rerouting of subglacial flow, small errors in the DEMs may also have the same effect on the modeled flow paths. We expand the hydraulic potential equation (5) to examine the perturbation in hydraulic head due to the errors in the surface and bed DEMs, as well as the possible effects of density variation in the ice column following *Creyts et al.* [2014] (see supporting information section S2). The perturbation analysis shows that the error in the DEMs contributes to 24 m of uncertainty in the hydraulic head averaged over the entire study region. This 24 m is equivalent to a 2.5% change in flotation fraction and represents the minimum resolution of the DEMs. Because of the high data density in the regions of subglacial rerouting, the uncertainty in these locations is smaller (13 m) than the average value over the study area. An increase of flotation fraction from $f = 1.0$ to $f = 1.11$ would result in a 98 m change in hydraulic head averaged across the study region. Therefore, the predicted rerouting of water flow between Nordenskiöld and Alángordliup is not a byproduct of the errors in the DEMs.

5. Discussion

5.1. Potential Impact on Seasonal Ice Velocity

While the pattern of surface meltwater delivery has recently been suggested to change ice flow velocity [*Bartholomew et al.*, 2010; *Colgan et al.*, 2011; *Hoffman et al.*, 2011; *Palmer et al.*, 2011], our results suggest that if water is delivered to critical areas of the bed, rerouting of drainage pathways can cause glaciers to respond differently to the same meltwater input. We investigate the impact of water rerouting on the glaciers transient response to melt by examining two snapshots of the summer ice motion from 16 July 2009 and 19 June 2010 (Figures 1b and 1c). These two snapshots represent the periods of greatest summer speedup measured that year. The velocity snapshots illustrate that the spatial pattern of the transient speedup varies substantially from year to year [*Joughin et al.*, 2013] (Figures 1b and 1c). When the subglacial water flow paths are overlain on these velocities, a qualitative spatial correlation between the velocity and drainage pathways emerges. This correlation suggests that the intraannual difference in the speedups pattern may be related to water piracy between Nordenskiöld and Alángordliup.

The 2009 summer velocity snapshot shows that the regions of greatest speedup ($>$100% of winter velocity) occur principally in the subglacial overdeepening in the upper catchment (Figure 6a). In contrast, the downstream region experiences a lower flow speedup of $<$40% of the winter velocity. The sharp transition of the flow speedup roughly aligns with an area near the adverse-sloped bed near the subglacial overdeepening. This general spatial pattern of the 2009 summer speedup shows strong similarity to the configuration of the subglacial drainage pathways at or near the ice overburden pressure ($f = 0.8$ and 1.0). The transition of the flow speedup coincides with the divergence of the Alángordliup subglacial water flow paths toward Nordenskiöld.

In contrast to the 2009 observations, the 2010 summer velocity snapshot shows that the regions of greatest summer speedup expand across the adverse-sloped bed farther downglacier (Figure 6b). The similarity between the spatial speedup pattern and the inferred drainage pathways when water pressure is excess of overburden ($f = 1.11$) suggests that the subglacial system is likely highly pressurized at this time. The 2010 melt season was anomalously warm and had higher surface melting in the ablation zone than in the melt season of 2009 [*Mernild et al.*, 2011; *Tedesco et al.*, 2011], so that an overpressured subglacial system could be responsible for this early and extensive transient speedup. Landsat imagery from around the time of greatest speed up reveals that many supraglacial lakes developed in late June 2010, approximately 2 weeks earlier than in 2009. The rapid supply of meltwater from supraglacial lake drainage events to the subglacial hydrologic system could have resulted in localized pressures above flotation. If such overpressurization occurs near the overdeepening, our results predict that it would lead to water piracy from Nordenskiöld to Alángordliup. The increase of subglacial water to Alángordliup may reduce the basal resistance in the downstream region and contribute to the transient summer speedup in the downstream region of Alángordliup observed in the 2010 velocity snapshot.

Because the three outlet glaciers are marine terminating, ocean-related forcing such as retreat of the grounding lines could potentially impact the glaciers surface velocity. When icebergs calve, the loss of resisting force may potentially trigger a surface velocity speedup of the inland ice [*Vieli and Nick*, 2011; *Joughin et al*., 2012; *Podrasky et al*., 2012]. The force perturbation from the grounding lines should be greatest at the ice sheet margin and decays with distance upglacier [*Cuffey and Paterson*, 2010]. However, the velocity in 2010 shows the opposite speedup variation at Alángordliup and Sarqardliup with lower speedup closer to the calving front than the upstream ice. Also, much of the differences in the transient summer speedups between 2009 and 2010 occurred in the interior of the ablation zone ($>$30 km from the ice termini) where the force perturbation related to grounding line changes may have decayed significantly. It is therefore more likely that the transient summer speedup in 2010 is associated with the reduction of basal resistance from hydrological changes at the bed coincident with a greater surface melt year. The net effect of these transient speedups on the annual ice motion is likely small [e.g., *Joughin et al*., 2008; *Tedstone et al*., 2015]. Nonetheless, our study indicate that the sensitivity for the Greenland ice sheet to subglacial water piracy means that the spatial distribution of the transient summer speedups can vary substantially from year to year depending on the subglacial hydrologic configuration.

5.2. Potential Impact on Water Budget Assessments

Water piracy between neighboring subglacial catchments also changes the hydrographic assessments of water budget for individual glaciers. Point measurements of hydrographs at proglacial rivers as well as salt and temperature budgets at fjord outlets have been used to infer the configurations of subglacial hydrologic system and their relationship with changes in ice velocity [*Mernild et al*., 2011; *Chandler et al*., 2013; *Cowton et al*., 2013; *Hasholt et al*., 2013] Changes in hydrograph shape and amplitude are often interpreted as a transition in the subglacial hydrologic system [e.g., *Swift et al*., 2005; *Jobard and Dzikowski*, 2006]. Most discharge budget analyses assume that the meltwater is confined within the ice catchment directly upstream of the sampling sites. While this assumption is realistic for small topographically constrained alpine catchments, our study suggests that the same assumption is not always valid for Greenland catchments where glaciers are less topographically constrained and have lower hydraulic gradients. Greenland-type glaciers are more likely to undergo water piracy between catchments than alpine-type glaciers [*Lindbäck et al*., 2015]. The tendency for Greenland glaciers to experience subglacial water rerouting means that the imbalance in the discharge budget analyses could imply changes in water transport in addition to changes in water storage [*Rennermalm et al*., 2012; *Lindbäck et al*., 2015; *Smith et al*., 2015]. Our findings suggest that both extents of the supraglacial catchments and the subglacial catchment are necessary to understand how discharge budgets reflect the water sources. In addition, detail measurements of subglacial topography and estimates of water pressure are necessary to determine the subglacial pathways for a catchment.

6. Conclusions

Our results show that changes in water pressure can potentially result in rerouting of subglacial flow between adjacent glaciers. By incrementing water pressure from 60 to 111% of the ice overburden pressure, we show that small changes in flotation fraction from 1.0 to 1.11 occur at critical locations at the bed can result in major subglacial flow rerouting. An increase of water pressure above flotation from $f = 1.0$ to 1.11 can potentially divert subglacial water flow between Nordenskiöld and Alángordliup. The diversion of subglacial water appears to correlate with the transient summer speedup in the high melt year of 2010 where water would create additional lubrication at the ice bed interface.

Subglacial flow paths are sensitive to the water pressure condition because it modifies the dependence of flow on topography. Water pressures in excess of the overburden pressure tend to drive flow in the direction of surface slope. In contrast, low pressures tend to steer water flow along bed slopes. The sensitivity of subglacial flow to variations in water pressure is not uniform across the ice catchment. Flow paths are more likely to reroute in regions where subtle changes in pressure impact a near-flat hydraulic potential surface. This difference is particularly important where bed slope is significant and adverse to the surface slopes, such as in areas of subglacial overdeepening where surface slopes tend to be subdued. In these adverse-sloped bed regions, water flow can periodically be rerouted between predominately bed slope and surface slope-dependent pathways when water pressure fluctuates. We predict that in our study region, subglacial flow reroutes from bed slope-directed flow toward Nordenskiöld to surface slope-directed flow toward

Alángordliup when water pressure increases above the local flotation pressure. Localized supply of meltwater from the ice surface, for example, through episodic and rapid supraglacial lake drainages could lead to the rerouting of subglacial flow in critical areas by increasing the water pressure locally. We suggest that catchment-scale rerouting of subglacial water may modify the spatial pattern of basal resistance. This change in resistance could lead to a more spatially extensive or restricted summer velocity speedup depending on the local effects on drainage. The surface velocity observation from 2010 summer provides potential support that the more extensive velocity speedup in the lower 30 km region of Alángordliup is a result of the rerouting of subglacial water from Nordenskiöld to Alángordliup.

Additionally, the rerouting of subglacial water flow has implications on the assessment of glacier water budgets. Piracy of water between neighboring subglacial water catchments can result in an imbalance between the local measurements of input surface runoff and output discharge at the ice sheet margin. In sum, our study demonstrates that the configuration of subglacial water flow paths beneath Greenland can evolve over time and is particularly sensitive to water pressure and its interaction with topography. Because our calculations assume steady state and uniform water input, we suggest that further investigations using dynamic models are needed to better assess the effects of topography and the critical locations for water rerouting relative to surface drainage in the Greenland ice sheet.

Acknowledgments

W.C. would like to thank I. Joughin for sharing the velocity data for the study regions. K.J. Tinto is gratefully acknowledged for her informative discussions on the interpolation and error analysis on the DEMs. The authors would also like to thank Bryn Hubbard and the anonymous reviewers for comments that greatly improved the manuscript. W.C. is supported by a NASA Earth and Space Science Fellowship NNX15AN28H. T.T.C is supported by a NSF grant ANT-1043481. R.E.B is supported by a NASA IceBridge grant NNX13AD25A. The fieldwork was funded through NSF OPP award ANT-0632292 for the Antarctica Gamburtsev Province Project. The Lamont-Doherty thickness data presented in the paper are available by contacting the corresponding author and will be available on the NSIDC website.

References

Ahlstrøm, A. P., J. J. Mohr, N. Reeh, E. L. Christensen, and R. L. Hooke (2005), Controls on the basal water pressure in subglacial channels near the margin of the Greenland ice sheet controls on the basal water pressure in subglacial channels near the margin of the Greenland ice sheet, *J. Glaciol.*, *51*, 443–450.

Alley, R. B., S. Anandakrishnan, C. R. Bentley, and N. Lord (1994), A water-piracy hypothesis for the stagnation of Ice Stream C, Antarctica, *Ann. Glaciol.*, *20*(1979), 187–194, doi:10.3189/172756494794587032.

Anandakrishnan, S., and R. B. Alley (1997), Stagnation of Ice Stream C, West Antarctica by water piracy, *Geophys. Res. Lett.*, *24*(3), 265–268, doi:10.1029/96GL04016.

Andrews, L. C., G. A. Catania, M. J. Hoffman, J. D. Gulley, M. P. Lüthi, C. Ryser, R. L. Hawley, and T. A. Neumann (2014), Direct observations of evolving subglacial drainage beneath the Greenland ice sheet, *Nature*, *514*(7520), 80–83, doi:10.1038/nature13796.

Bamber, J. L., et al. (2013), A new bed elevation dataset for Greenland, *Cryosphere*, *7*(2), 499–510, doi:10.5194/tc-7-499-2013.

Banwell, A. F., I. C. Willis, and N. S. Arnold (2013), Modeling subglacial water routing at Paakitsoq, W Greenland, *J. Geophys. Res. Earth Surf.*, *118*, 1282–1295, doi:10.1002/jgrf.20093.

Bartholomaus, T. C., R. S. Anderson, and S. P. Anderson (2008), Response of glacier basal motion to transient water storage, *Nat. Geosci.*, *1*(1), 33–37, doi:10.1038/ngeo.2007.52.

Bartholomew, I. D., P. Nienow, A. Sole, D. Mair, T. Cowton, M. A. King, and S. Palmer (2011), Seasonal variations in Greenland Ice Sheet motion: Inland extent and behaviour at higher elevations, *Earth Planet. Sci. Lett.*, *307*(3–4), 271–278, doi:10.1016/j.epsl.2011.04.014.

Bartholomew, I., P. Nienow, D. Mair, A. Hubbard, M. A. King, and A. Sole (2010), Seasonal evolution of subglacial drainage and acceleration in a Greenland outlet glacier, *Nat. Geosci.*, *3*(6), 408–411, doi:10.1038/ngeo863.

Bartholomew, I., P. Nienow, A. Sole, D. Mair, T. Cowton, and M. A. King (2012), Short-term variability in Greenland ice sheet motion forced by time-varying meltwater drainage: Implications for the relationship between subglacial drainage system behavior and ice velocity, *J. Geophys. Res.*, *117*, F03002, doi:10.1029/2011JF002220.

Bingham, R. G., P. W. Nienow, M. J. Sharp, and S. Boon (2005), Subglacial drainage processes at a High Arctic polythermal valley glacier, *J. Glaciol.*, *51*, 15–24, doi:10.3189/172756505781829520.

Box, J. E., and W. Colgan (2013), Greenland ice sheet mass balance reconstruction. Part III: Marine ice loss and total mass balance (1840–2010), *J. Clim.*, *26*, 6990–7002, doi:10.1175/JCLI-D-12-00546.1.

Carter, S. P., H. A. Fricker, and M. R. Siegfried (2013), Evidence of rapid subglacial water piracy under Whillans Ice Stream, West Antarctica, *J. Glaciol.*, *59*(218), 1147–1162, doi:10.3189/2013JoG13J085.

Chandler, D. M., et al. (2013), Evolution of the subglacial drainage system beneath the Greenland ice sheet revealed by tracers, *Nat. Geosci.*, *6*(3), 195–198, doi:10.1038/ngeo1737.

Colgan, W., H. Rajaram, R. Anderson, K. Steffen, T. Phillips, I. Joughin, H. J. Zwally, and W. Abdalati (2011), The annual glaciohydrology cycle in the ablation zone of the Greenland ice sheet: Part 1. Hydrology model, *J. Glaciol.*, *57*(204), 697–709, doi:10.3189/002214311797409668.

Cook, S. J., and D. A. Swift (2012), Subglacial basins: Their origin and importance in glacial systems and landscapes, *Earth Sci. Rev.*, *115*(4), 332–372, doi:10.1016/j.earscirev.2012.09.009.

Cowton, T., P. Nienow, A. Sole, J. Wadham, G. Lis, I. Bartholomew, D. Mair, and D. Chandler (2013), Evolution of drainage system morphology at a land-terminating Greenlandic outlet glacier, *J. Geophys. Res. Earth Surf.*, *118*, 29–41, doi:10.1029/2012JF002540.

Cressie, N. (1993), *Statistics for Spatial Data*, Revised ed., Wiley, New York.

Creyts, T. T., and C. G. Schoof (2009), Drainage through subglacial water sheets, *J. Geophys. Res.*, *114*, F04008, doi:10.1029/2008JF001215.

Creyts, T. T., G. K. C. Clarke, and M. Church (2013), Evolution of subglacial overdeepenings in response to sediment redistribution and glaciohydraulic supercooling, *J. Geophys. Res. Earth Surf.*, *118*, 423–446, doi:10.1002/jgrf.20033.

Creyts, T. T., et al. (2014), Freezing of ridges and water networks preserves the Gamburtsev Subglacial Mountains for millions of years, *Geophys. Res. Lett.*, *41*, 8114–8122, doi:10.1002/2014GL061491.

Cuffey, K., and W. S. Paterson (2010), *The Physics of Glaciers*, 4th ed., Butterworth-Heinemann/Elsevier, Oxford, U. K.

Das, S. B., I. Joughin, M. D. Behn, I. M. Howat, M. A. King, D. Lizarralde, and M. P. Bhatia (2008), Fracture propagation to the base of the Greenland ice sheet during supraglacial lake drainage, *Science*, *320*(5877), 778–781, doi:10.1126/science.1153360.

den Hertog, D., J. P. C. Kleijnen, and A. Y. D. Siem (2006), The correct Kriging variance estimated by bootstrapping, *J. Oper. Res. Soc.*, *57*(4), 400–409, doi:10.1057/palgrave.jors.2601997.

Deutsch, C. V., and A. G. Journel (1997), *GSLIB-Geostatistical Software Library and User's Manual*, 2nd ed., 369 p., Oxford Univ. Press, New York.
Echelmeyer, K., T. S. Clarke, and W. D. Harrison (1991), Surficial glaciology of Jakoshavns isbrae, west Greenland: 1. Surface morphology, *J. Glaciol.*, *37*, 368–382.
Fettweis, X., M. Tedesco, M. van den Broeke, and J. Ettema (2011), Melting trends over the Greenland ice sheet (1958–2009) from spaceborne microwave data and regional climate models, *Cryosphere*, *5*(2), 359–375, doi:10.5194/tc-5-359-2011.
Flowers, G. E., and G. K. C. Clarke (1999), Surface and bed topography of Trapridge Glacier, Yukon Territory, Canada: Digital elevation models and derived hydraulic geometry, *J. Glaciol.*, *45*(149), 165–174.
Fudge, T. J., J. T. Harper, N. F. Humphrey, and W. T. Pfeffer (2009), Rapid glacier sliding, reverse ice motion and subglacial water pressure during an autumn rainstorm, *Ann. Glaciol.*, *50*(52), 101–108, doi:10.3189/172756409789624247.
Gogineni, S., D. Tammana, J. Stiles, C. Allen, and K. Jezek (2001), Coherent radar ice thickness measurements over the Greenland ice sheet, *J. Geophys. Res.*, *106*(D24), 33,761–33,772, doi:10.1029/2001JD900183.
Gudmundsson, G. H. (2003), Transmission of basal variability to a glacier surface, *J. Geophys. Res.*, *108*(B5), 2253, doi:10.1029/2002JB002107.
Hagen, J. O., B. Etzelmüller, and A. M. Nuttall (2000), Runoff and drainage pattern derived from digital elevation models, Finsterwalderbreen, Svalbard, *Ann. Glaciol.*, *31*, 147–152, doi:10.3189/172756400781819879.
Hanna, E., et al. (2013), Ice-sheet mass balance and climate change, *Nature*, *498*(7452), 51–59, doi:10.1038/nature12238.
Harper, J. T., N. F. Humphrey, W. T. Pfeffer, T. Fudge, and S. O. Neel (2005), Evolution of subglacial water pressure along a glacier's length, *Ann. Glaciol.*, *40*(1981), 31–36.
Hasholt, B., A. Bech Mikkelsen, M. Holtegaard Nielsen, and M. Andreas Dahl Larsen (2013), Observations of runoff and sediment and dissolved loads from the Greenland ice sheet at Kangerlussuaq, west Greenland, 2007 to 2010, *Z. Geomorphol. Suppl. Issues*, *57*(2), 3–27, doi:10.1127/0372-8854/2012/S-00121.
Hélière, F., C. Lin, H. Corr, and D. Vaughan (2007), Radio echo sounding of Pine Island glacier, west Antarctica: Aperture synthesis processing and analysis of feasibility from space, *IEEE Geosci. Remote Sens. Lett.*, *45*(8), 2573–2582.
Hewitt, I. J. (2013), Seasonal changes in ice sheet motion due to melt water lubrication, *Earth Planet. Sci. Lett.*, *371–372*, 16–25, doi:10.1016/j.epsl.2013.04.022.
Hoffman, M. J., G. A. Catania, T. A. Neumann, L. C. Andrews, and J. A. Rumrill (2011), Links between acceleration, melting, and supraglacial lake drainage of the western Greenland ice sheet, *J. Geophys. Res.*, *116*, F04035, doi:10.1029/2010JF001934.
Hooke, R., and V. Pohjola (1994), Hydrology of a segment of a glacier situated in an overdeepening, Storglaciaren, Sweden, *J. Glaciol.*, *40*(134), 140–148.
Howat, I. M., A. Negrete, and B. E. Smith (2014), The Greenland Ice Mapping Project (GIMP) land classification and surface elevation datasets, *Cryosphere Discuss.*, *8*(1), 453–478, doi:10.5194/tcd-8-453-2014.
Iken, A. (1981), The effect of the subglacial water pressure at the sliding velocity of a glacier in an idealized numerical model, *J. Glaciol.*, *27*(97), 407–421.
Iken, A., and R. A. Bindschadler (1986), Combined measurements of subglacial water pressure and surface velocity at Findelengletscher, Switzerland, conclusions about drainage system and sliding mechanism, *J. Glaciol.*, *32*, 101–119.
Iken, A., and M. Truffer (1997), The relationship between subglacial water pressure and velocity of Findelengletscher, Switzerland, during its advance and retreat, *J. Glaciol.*, *43*(144), 328–338.
Intergovernmental Panel on Climate Change (2013), Summary for policy, in *Climate Change 2013: The Physical Science Basis. Contribution of Working Group I to the Fifth Assessment Report of the Intergovernmental Panel on Climate Change*, pp. 1535, Cambridge Univ. Press, Cambridge, U. K., and New York.
Jezek, K., E. Rodríguez, P. Gogineni, A. Freeman, J. Curlander, X. Wu, J. Paden, and C. Allen (2006), Glaciers and ice sheets mapping orbiter concept, *J. Geophys. Res.*, *111*, E06S20, doi:10.1029/2005JE002572.
Jobard, S., and M. Dzikowski (2006), Evolution of glacial flow and drainage during the ablation season, *J. Hydrol.*, *330*(3–4), 663–671, doi:10.1016/j.jhydrol.2006.04.031.
Joughin, I., S. B. Das, M. A. King, B. E. Smith, I. M. Howat, and T. Moon (2008), Seasonal speedup along the western flank of the Greenland ice sheet, *Science*, *320*(5877), 781–783, doi:10.1126/science.1153288.
Joughin, I., B. E. Smith, I. M. Howat, T. Scambos, and T. Moon (2010), Greenland flow variability from ice-sheet-wide velocity mapping, *J. Glaciol.*, *56*(197), 415–430, doi:10.3189/002214310792447734.
Joughin, I., R. B. Alley, and D. M. Holland (2012), Ice-sheet response to oceanic forcing, *Science*, *338*(6111), 1172–6, doi:10.1126/science.1226481.
Joughin, I., S. B. Das, G. E. Flowers, M. D. Behn, R. B. Alley, M. A. King, B. E. Smith, J. L. Bamber, M. R. van den Broeke, and J. H. van Angelen (2013), Influence of ice-sheet geometry and supraglacial lakes on seasonal ice-flow variability, *Cryosphere*, *7*(4), 1185–1192, doi:10.5194/tc-7-1185-2013.
Karlsson, N. B., and D. Dahl-Jensen (2015), Response of the large-scale subglacial drainage system of North East Greenland to surface elevation changes, *Cryosphere*, *9*, 1465–1479, doi:10.5194/tcd-9-719-2015.
Khan, S. A., et al. (2014), Sustained mass loss of the northeast Greenland ice sheet triggered by regional warming, *Nat. Clim. Change*, *4*, 292–299, doi:10.1038/nclimate2161.
Lawson, D. E., J. C. Strasser, E. B. Evenson, R. B. Alley, G. J. Larson, and S. A. Arcone (1998), Glaciohydraulic supercooling: A freeze-on mechanism to create stratified, debris-rich basal ice: I. Field evidence, *J. Glaciol.*, *44*(148), 547–562.
Lewis, S. M., and L. C. Smith (2009), Hydrologic drainage of the Greenland ice sheet, *Hydrol. Process.*, *23*(14), 2004–2011, doi:10.1002/hyp.7343.
Lindbäck, K., R. Pettersson, A. L. Hubbard, S. H. Doyle, D. van As, A. B. Mikkelsen, and A. A. Fitzpatrick (2015), Subglacial water drainage, storage, and piracy beneath the Greenland ice sheet, *Geophys. Res. Lett.*, *42*, 7606–7614, doi:10.1002/2015GL065393.
Livingstone, S. J., C. D. Clark, and J. Woodward (2013), Predicting subglacial lakes and meltwater drainage pathways beneath the Antarctic and Greenland ice sheets, *Cryosphere Discuss.*, *7*(2), 1177–1213, doi:10.5194/tcd-7-1177-2013.
Mair, D., P. Nienow, M. J. Sharp, T. Wohlleben, and I. Willis (2002), Influence of subglacial drainage system evolution on glacier surface motion: Haut Glacier d'Arolla, Switzerland, *J. Geophys. Res.*, *107*(B8), 2175, doi:10.1029/2001JB000514.
Meierbachtol, T., J. Harper, and N. Humphrey (2013), Basal drainage system response to increasing surface melt on the Greenland ice sheet, *Science*, *341*(6147), 777–779, doi:10.1126/science.1235905.
Mernild, S. H., T. L. Mote, and G. E. Liston (2011), Greenland ice sheet surface melt extent and trends: 1960–2010, *J. Glaciol.*, *57*(204), 621–628, doi:10.3189/002214311797409712.
Palmer, S., A. Shepherd, P. Nienow, and I. Joughin (2011), Seasonal speedup of the Greenland ice sheet linked to routing of surface water, *Earth Planet. Sci. Lett.*, *302*(3–4), 423–428, doi:10.1016/j.epsl.2010.12.037.

Pimentel, S., and G. E. Flowers (2010), A numerical study of hydrologically driven glacier dynamics and subglacial flooding, *Proc. R. Soc. A Math. Phys. Eng. Sci.*, *467*(2126), 537–558, doi:10.1098/rspa.2010.0211.

Podrasky, D., M. Truffer, M. Fahnestock, J. M. Amundson, R. Cassotto, and I. Joughin (2012), Outlet glacier response to forcing over hourly to interannual timescales, Jakobshavn Isbræ, Greenland, *J. Glaciol.*, *58*(212), 1212–1226, doi:10.3189/2012JoG12J065.

Rennermalm, A. K., L. C. Smith, V. W. Chu, R. R. Forster, J. E. Box, and B. Hagedorn (2012), Proglacial river stage, discharge, and temperature datasets from the Akuliarusiarsuup Kuua River northern tributary, Southwest Greenland, 2008–2011, *Earth Syst. Sci. Data*, *4*(1), 1–12, doi:10.5194/essd-4-1-2012.

Rignot, E., and P. Kanagaratnam (2006), Changes in the velocity structure of the Greenland ice sheet, *Science*, *311*(5763), 986–990, doi:10.1126/science.1121381.

Rothlisberger, H. (1972), Water pressure in intra- and subglacial channels, *J. Glaciol.*, *11*(62), 7–13.

Schoof, C. (2010), Ice-sheet acceleration driven by melt supply variability, *Nature*, *468*(7325), 803–806, doi:10.1038/nature09618.

Sergienko, O. V. (2013), Glaciological twins: Basally controlled subglacial and supraglacial lakes, *J. Glaciol.*, *59*(213), 3–8, doi:10.3189/2013JoG12J040.

Shepherd, A., et al. (2012), A reconciled estimate of ice-sheet mass balance, *Science*, *338*(6111), 1183–1189, doi:10.1126/science.1228102.

Shreve, R. (1972), Movement of water in glaciers, *J. Glaciol.*, *11*(62), 205–214.

Smith, L. C., et al. (2015), Efficient meltwater drainage through supraglacial streams and rivers on the southwest Greenland ice sheet, *Proc. Natl. Acad. Sci. U.S.A.*, *112*(4), 1001–1006, doi:10.1073/pnas.1413024112.

Sole, A. J., D. W. Mair, P. W. Nienow, I. D. Bartholomew, M. A. King, M. J. Burke, and I. R. Joughin (2011), Seasonal speedup of a Greenland marine-terminating outlet glacier forced by surface melt-induced changes in subglacial hydrology, *J. Geophys. Res.*, *116*, F03014, doi:10.1029/2010JF001948.

Sugiyama, S., and G. H. Gudmundsson (2004), Short-term variations in glacier flow controlled by subglacial water pressure at Lauteraargletscher, Bernese Alps, Switzerland, *J. Glaciol.*, *50*, 353–362, doi:10.3189/172756504781829846.

Sundal, A. V., A. Shepherd, P. Nienow, E. Hanna, S. Palmer, and P. Huybrechts (2011), Melt-induced speed-up of Greenland ice sheet offset by efficient subglacial drainage, *Nature*, *469*(7331), 521–524, doi:10.1038/nature09740.

Swift, D. A., P. W. Nienow, T. B. Hoey, and D. W. F. Mair (2005), Seasonal evolution of runoff from Haut Glacier d'Arolla, Switzerland and implications for glacial geomorphic processes, *J. Hydrol.*, *309*(1–4), 133–148, doi:10.1016/j.jhydrol.2004.11.016.

Tarboton, D. G. (1997), A new method for the determination of flow directions and upslope areas in grid digital elevation models, *Water Resour. Res.*, *33*(2), 309–319, doi:10.1029/96WR03137.

Tedesco, M., X. Fettweis, M. R. van den Broeke, R. S. W. van de Wal, C. J. P. P. Smeets, W. J. van de Berg, M. C. Serreze, and J. E. Box (2011), The role of albedo and accumulation in the 2010 melting record in Greenland, *Environ. Res. Lett.*, *6*(1), 014005, doi:10.1088/1748-9326/6/1/014005.

Tedstone, A. J., P. W. Nienow, N. Gourmelen, and A. J. Sole (2014), Greenland ice sheet annual motion insensitive to spatial variations in subglacial hydraulic structure, *Geophys. Res. Lett.*, *41*, 8910–8917, doi:10.1002/2014GL062386.

Tedstone, A. J., P. W. Nienow, N. Gourmelen, A. Dehecq, D. Goldberg, and E. Hanna (2015), Decadal slowdown of a land-terminating sector of the Greenland ice sheet despite warming, *Nature*, *526*(7575), 692–695, doi:10.1038/nature15722.

van de Wal, R. S. W., W. Boot, M. R. van den Broeke, C. J. P. P. Smeets, C. H. Reijmer, J. J. A. Donker, and J. Oerlemans (2008), Large and rapid melt-induced velocity changes in the ablation zone of the Greenland ice sheet, *Science*, *321*(5885), 111–113, doi:10.1126/science.1158540.

van den Broeke, M., J. Bamber, J. Ettema, E. Rignot, E. Schrama, W. J. van de Berg, E. van Meijgaard, I. Velicogna, and B. Wouters (2009), Partitioning recent Greenland mass loss, *Science*, *326*(5955), 984–986, doi:10.1126/science.1178176.

Vaughan, D. G., H. F. J. Corr, A. M. Smith, H. D. Pritchard, and A. Shepherd (2008), Flow-switching and water piracy between Rutford Ice Stream and Carlson Inlet, West Antarctica, *J. Glaciol.*, *54*(184), 41–48.

Vieli, A., and F. M. Nick (2011), Understanding and modelling rapid dynamic changes of tidewater outlet glaciers: Issues and implications, *Surv. Geophys.*, *32*(4–5), 437–458, doi:10.1007/s10712-011-9132-4.

Werder, M. A., I. J. Hewitt, C. G. Schoof, and G. E. Flowers (2013), Modeling channelized and distributed subglacial drainage in two dimensions, *J. Geophys. Res. Earth Surf.*, *118*, 2140–2158, doi:10.1002/jgrf.20146.

Willis, I. C., C. D. Fitzsimmons, K. Melvold, L. M. Andreassen, and R. H. Giesen (2012), Structure, morphology and water flux of a subglacial drainage system, Midtdalsbreen, Norway, *Hydrol. Process.*, *26*(25), 3810–3829, doi:10.1002/hyp.8431.

Wolovick, M. J., R. E. Bell, T. T. Creyts, and N. Frearson (2013), Identification and control of subglacial water networks under Dome A, Antarctica, *J. Geophys. Res. Earth Surf.*, *118*, 140–154, doi:10.1029/2012JF002555.

Wright, A. P., M. J. Siegert, A. M. Le Brocq, and D. B. Gore (2008), High sensitivity of subglacial hydrological pathways in Antarctica to small ice-sheet changes, *Geophys. Res. Lett.*, *35*, L17504, doi:10.1029/2008GL034937.

Zwally, H. J., W. Abdalati, T. Herring, K. Larson, J. Saba, and K. Steffen (2002), Surface melt-induced acceleration of Greenland ice-sheet flow, *Science*, *297*(5579), 218–222, doi:10.1126/science.1072708.